

## Research Paper

# Integrin $\alpha\beta6$ -specific therapy for pancreatic cancer developed from foot-and-mouth-disease virus

Kate M. Moore<sup>1</sup>, Ami Desai<sup>1</sup>, Bea de Luxán Delgado<sup>1</sup>, Sara Maria David Trabulo<sup>1</sup>, Claire Reader<sup>1</sup>, Nicholas F. Brown<sup>1</sup>, Elizabeth R. Murray<sup>1</sup>, Adam Brentnall<sup>2</sup>, Philip Howard<sup>3</sup>, Luke Masterson<sup>3</sup>, Francesca Zammarchi<sup>4</sup>, John A. Hartley<sup>5</sup>, Patrick H. van Berkel<sup>1</sup>, John F. Marshall<sup>1</sup>✉

1. Barts Cancer Institute, Queen Mary University of London, John Vane Science Centre, Charterhouse Square, London EC1M 6BQ, UK.
2. Cancer Research UK Centre for Epidemiology, Mathematics and Statistics, Wolfson Institute of Preventative Medicine, Queen Mary University of London, Charterhouse Square, London EC1M 6BQ, UK.
3. Spirogen, QMB Innovation Centre, 42 New Road, London E1 2AX, UK.
4. ADC Therapeutics (UK) Ltd, QMB Innovation Centre, 42 New Road, London E1 2AX, UK.
5. Cancer Research UK Drug-DNA Interactions Research Group, University College London Cancer Institute, 72 Huntley Street, London WC1E 6BT, U.K.

✉ Corresponding author: Professor John F. Marshall, Centre for Tumour Biology, Barts Cancer Institute, Queen Mary University of London, John Vane Science Centre, Charterhouse Square, London EC1M 6BQ, UK (Tel: +44 (0) 20 7882 3580, e-mail: j.f.marshall@qmul.ac.uk).

© The author(s). This is an open access article distributed under the terms of the Creative Commons Attribution License (<https://creativecommons.org/licenses/by/4.0/>). See <http://ivyspring.com/terms> for full terms and conditions.

Received: 2019.07.24; Accepted: 2019.12.16; Published: 2020.02.12

## Abstract

**Goals of investigation:** The 5-year survival rate for pancreatic ductal adenocarcinoma (PDAC) has remained at <5% for decades because no effective therapies have been identified. Integrin  $\alpha\beta6$  is overexpressed in most PDAC and represents a promising therapeutic target. Thus, we attempted to develop an  $\alpha\beta6$ -specific peptide-drug conjugate (PDC) for therapy of PDAC.

**Methodology:** We conjugated the DNA-binding pyrrolobenzodiazepine (PBD)-based payload SG3249 (tesirine) to an  $\alpha\beta6$ -specific 20mer peptide from the VP1 coat protein of foot-and-mouth-disease virus (FMDV) (forming conjugate SG3299) or to a non-targeting peptide (forming conjugate SG3511). PDCs were tested for specificity and toxicity on  $\alpha\beta6$ -negative versus-positive PDAC cells, patient-derived cell lines from tumor xenografts, and on two different *in vivo* models of PDAC. Immunohistochemical analyses were performed to establish therapeutic mechanism.

**Results:** The  $\alpha\beta6$ -targeted PDC SG3299 was significantly more toxic (up to 78-fold) for  $\alpha\beta6$ -expressing versus  $\alpha\beta6$ -negative PDAC cell lines *in vitro*, and achieved significantly higher toxicity at equal dose than the non-targeted PDC SG3511 (up to 15-fold better). Moreover, SG3299 eliminated established (100mm<sup>3</sup>) Capan-1 PDAC human xenografts, extending the lifespan of mice significantly (P=0.005). Immunohistochemistry revealed SG3299 induced DNA damage and apoptosis (increased  $\gamma$ H2AX and cleaved caspase 3, respectively) associated with significant reductions in proliferation (Ki67),  $\beta6$  expression and PDAC tumour growth.

**Conclusions:** The FMDV-peptide drug conjugate SG3299 showed  $\alpha\beta6$ -selectivity *in vitro* and *in vivo* and can specifically eliminate  $\alpha\beta6$ -positive cancers, providing a promising new molecular-specific therapy for pancreatic cancer.

Key words: integrin,  $\alpha\beta6$ , PDAC, peptide-drug conjugate

## Introduction

Pancreatic ductal adenocarcinoma (PDAC) is the fourth most common cause of cancer-related deaths [1] with a 5-year survival rate of less than 5% [2],

predominantly due to clinical signs of disease occurring late in disease progression, often after metastasis has occurred. Current treatment options

are extremely limited, with surgical resection and chemotherapy only effective in cases that are detected early and when disease is restricted to the pancreas. Combination chemotherapy strategies such as FOLFIRINOX (fluorouracil, leucovorin, irinotecan and oxaliplatin) and gemcitabine with nab-paclitaxel have significantly improved survival compared to gemcitabine, the previous standard of care for PDAC [3, 4]. However, these improvements amount to less than five months additional survival for patients who have metastatic disease, who are the majority of patients. The incidence of pancreatic cancer is increasing and is predicted to be the second highest cause of cancer-death in the USA by 2030 [5]. Thus, there remains an urgent unmet clinical need to develop effective targeted therapies.

Integrins are heterodimeric transmembrane receptors which mediate many biological functions including adhesion, migration, invasion, growth, survival and differentiation of cells [6]. Deregulation of integrin expression or signaling is associated with cancer development and metastasis. Integrin  $\alpha\beta6$  is overexpressed in over a third of carcinomas [7] in a variety of cancers including breast [8], cervical [9], colon [10], and non-small cell lung cancer [11], where its expression correlates with poor overall survival. We [12], and others [13,14], have reported that integrin  $\alpha\beta6$  is also overexpressed in most PDAC, whereas it is low or absent in normal pancreas, making  $\alpha\beta6$  a biomarker for disease but also a potential therapeutic target. In fact, we have shown antibody blockade of  $\alpha\beta6$  in human pancreas xenografts and mouse syngeneic tumours significantly slowed the growth of established tumours *in vivo* and increased survival [12]. In this study, we sought to deliver a cytotoxic drug specifically to kill  $\alpha\beta6$ -expressing pancreatic cancer cells *in vivo*.

To achieve cell-specific delivery of drugs requires a molecular-specific vector conjugated to a cytotoxic warhead. In earlier studies [7,15,16] we discovered that a 20 amino-acid sequence NAVPNLR GDLQVLAQKVART (termed A20FMDV2) from the VP1 coat protein of the O<sub>1</sub> BFS serotype of foot-and-mouth-disease-virus (FMDV), bound specifically and with high affinity (<1 nM) only to integrin  $\alpha\beta6$ , resulting in  $\alpha\beta6$ -dependent internalisation. Therefore we conjugated A20FMDV2, modified to include an N-terminal biotin and a C-terminal cysteine, to a cytotoxic payload, SG3249 (tesirine) [17]. Tesirine is comprised of a cathepsin B-cleavable valine-alanine linker conjugated to a pyrrolbenzodiazepine (PBD) warhead, SG3199. SG3199 is a potent PBD dimer toxin which covalently cross-links DNA in the minor groove, preventing replication and resulting in cell death [18]. Tesirine is currently being tested in clinical

trials conjugated to monoclonal antibodies to CD25 (NCT02432235; NCT02588092), CD19 (NCT02669017; NCT02669264), PSMA (NCT02991911) and DLL3 (NCT01901653) [19].

To our knowledge, no drugs that target  $\alpha\beta6$  in cancer are currently in pre-clinical development. We show here for the first time that by conjugating tesirine to the FMDV-derived peptide A20FMDV2 to create SG3299, we can selectively direct the DNA damaging activity of the PBD dimer to  $\alpha\beta6$ -overexpressing tumors and completely eliminate, or prevent development of, established pancreatic cancer xenografts. We suggest SG3299 is a promising new therapy for PDAC and many other carcinomas that upregulate  $\alpha\beta6$ .

## Materials & Methods

Additional methods details are described in Supplementary Methods.

### Chemical structures and synthesis

A20FMDV2 and non-targeting (NT) peptides, modified to include N-terminal biotinylation and a C-terminal cysteine which does not affect specificity (see below), were obtained from Peptide Synthetics (>95% purity; Peptide Protein Research Ltd, Hampshire, UK). A20FMDV2 [7, 15,16] and SG3199 [17] have been characterised previously; SG3249 and SG3199 were prepared as described [17]. Drugs were prepared as 1mM stocks in 100% DMSO, aliquoted and frozen at -20°C. Samples were thawed and diluted directly into PBS; the PBS only no-drug controls had equivalent concentrations of DMSO added. See Supplementary Figure S1 for conjugate structures and Supplementary Methods for conjugation procedures and analytical liquid chromatography /mass spectrometry (LC/MS) conditions for reaction monitoring, HPLC purity determination and manufacture of SG3511 and SG3299.

### Cell culture

A375P-Puro and A375P- $\beta6$  cell lines were developed in-house and have been characterized previously [15]. All other cell lines were provided by colleagues in Barts Cancer Institute. All cell lines were authenticated by LGC STR profiling (data not shown) and utilised within 6 months of resuscitation. A375P puro, A375P $\beta6$ , Panc1 and Colo357 cell lines were grown in DMEM+10%FBS. Capan-1 and Panc0403 cells were cultured in RPMI+10%FBS. PS1 cells were grown in DMEM:HamsF12+10%FBS. PANC354, PANC253 and PANC215 cells derived from 3 human PDX PDAC models were a generous gift from Professor James Eshleman (John Hopkins University, USA) and were cultured as previously described [20].

### Sphere-forming assay

500 cells/well of PANC354, PANC253 and PANC215 cells (hereafter termed 354, 253 & 215) were grown as adherent cells in 6-well plates. After 24h cells were treated with 1 nM, 10 nM, 50 nM, 100 nM and 500 nM PDCs or control containing DMSO. After 3 days, cells were collected and re-seeded at  $8 \times 10^3$  cells/well of a 24-well plate ( $n=5-6$  wells/treatment). After 10 days the number of spheres were counted. Photographs of spheres after 10 days were taken using an Olympus CKX31 inverted microscope and camera (Olympus Corporation, Japan) at  $\times 4$  magnification.

### Human tumor xenograft models

All animal experiments followed UK Home Office Guidelines. 8-week old female CD1Nu/Nu-mice (Charles River, UK) were inoculated subcutaneously with  $2 \times 10^6$  A375Ppuro, A375P $\beta 6$  or Capan-1 cells in 200  $\mu$ l of PBS. For PDAC/ stellate xenograft studies  $1 \times 10^6$  Panc0403 were co-injected with  $2 \times 10^6$  PS1 pancreatic stellate cells in PBS:Matrigel (2:1 ratio) into 8-week old female CD1Nu/Nu-mice. Mice were randomized into treatment groups once the starting tumor volume reached  $\sim 100$  mm<sup>3</sup>. Mice received either tri-weekly intraperitoneal injections (10  $\mu$ g/kg in 200  $\mu$ l of PBS) or bi-weekly intraperitoneal injections (20 or 25  $\mu$ g/kg in 200  $\mu$ l of PBS) for 4-5 weeks of NT-peptide control, A20FMDV2, SG3199, SG3511 or SG3299 ( $n=4-8$ /treatment). PBS control contained the equivalent amount of DMSO vehicle as peptide treatments. Tumors were measured with calipers bi-weekly in two directions and tumor volume calculated using the formula (width<sup>2</sup>  $\times$  length)/2. Animals were weighed at least bi-weekly to calculate accurate dosing and also observed for behavioural changes as a measure of possible toxicity. Tumors, organs and tissues were harvested at the end of each study for immunohistochemical analyses. In addition, some Capan-1 tumors, tissues and organs ( $n=3$ /treatment) were also harvested after 11 days (after 3 treatments) when treated with 25  $\mu$ g/kg bi-weekly.

### Peptide-drug conjugate serum stability assay

8-week old female CD1Nu/Nu-mice were treated with 20  $\mu$ g/kg SG3299 in 200  $\mu$ l of PBS by intraperitoneal injection for 2 minutes, 5 minutes, 15 minutes or 60 minutes. Untreated animals served as controls ( $n=4$ /condition). At the end of each time point, blood was collected via cardiac puncture under terminal anaesthesia and allowed to coagulate overnight at 4°C. Serum from each sample was then isolated by centrifugation at 1000 g for 20 minutes. The serum concentration of SG3299 was subsequently determined by enzyme-linked immunosorbent assay

(ELISA). In brief, peptide-drug conjugate was captured with 1.5  $\mu$ g/ml immobilised  $\alpha$ -PBD antibody (14B3-B7, ADC Therapeutics) synthesised as described [21]. Peptide-drug conjugate was then detected by incubation with Streptavidin-HRP (N200, Thermo Fisher) followed by the addition of 3,3',5,5'-Tetramethylbenzidine (TMB) substrate (34028, Thermo Fisher), neutralisation with 1M HCl, and measurement of absorbance at 450 nm minus absorbance at 620 nm. SG3299 concentration was determined by subtraction of absorbance readings from untreated mice and interpolation relative to reconstituted SG3299 standards of known concentration in GraphPad Prism software (Systat Software, San Jose, CA, USA).

### Immunohistochemical analysis

Immunohistochemistry utilized 4  $\mu$ m, formalin-fixed, paraffin-embedded serial sections of tumors. Tumor sections were stained for molecules of interest including epithelial markers pan-cytokeratin (CK) (M3515, DAKO) and E-cadherin (610181, BD Bioscience), marker of DNA damage  $\gamma$ H2AX (AB22551, Abcam), proliferation marker Ki67 (AB92742, Abcam),  $\alpha$ v $\beta 6$  (mAb 6.2E2, Biogen Idec), apoptotic marker cleaved-caspase 3 (9661, Cell Signaling Technology), endomucin for detection of endothelial cells (SC-53941 V.5C7, Santa Cruz), vimentin (V5255, Sigma) for detection of stromal mesenchymal cells (mostly fibroblasts) and  $\alpha$ -sma (M0581 clone 1A4, DAKO) for detection of activated fibroblasts/ stellate cells. The protocol used for  $\alpha$ v $\beta 6$  integrin was described previously [8]. Staining for CK and  $\alpha$ v $\beta 6$  was performed manually, all other staining was performed using the DISCOVERY XT automated IHC research slide staining system (Ventana Medical Systems Inc.).

### Statistical analysis

IC<sub>50</sub> values for *in vitro* analyses were obtained using GraphPad Prism software (Systat Software, San Jose, CA, USA). For 2 variables, data were analysed using an unpaired two-tailed student t-test and for 3 or more variables data were analysed using one-way ANOVA with Bonferroni's Multiple Comparison Test using Prism GraphPad software.

For tumor xenograft models, individual growth curves were plotted and a linear mixed model [22] was used to test for differences between treatment arms, fitted by maximum likelihood using the nlme package in the statistical software R 3.1.1 [23]. P values are from Wald tests. All statistical tests were two-sided. Error bars in all experiments represent standard deviation (SD) in *in vitro* studies and standard error of the mean (SEM) in *in vivo* studies.

**Table 1.** Peptide-drug conjugate cytotoxicity *in vitro*

Cell Line	$\alpha\text{v}\beta 6$ status	Drug/ Peptide drug conjugate(PDC) (IC <sub>50</sub> nM) <sup>1</sup>			PDC $\alpha\text{v}\beta 6$ Specificity Ratio <sup>2</sup>
		SG3199	SG3511	SG3299	
A375Ppuro	Negative	0.09 ± 0.07	101.08 ± 98.63	30.63 ± 18.75	3.30
A375Pβ6	Positive	0.11 ± 0.08	80.68 ± 41.65	5.37 ± 5.23	15.02
Capan-1	Positive	0.09 ± 0.08	11.72 ± 10.65	4.19 ± 3.76	2.80
Colo357	Positive	0.06 ± 0.05	24.57 ± 6.69	2.24 ± 1.59	10.97
Panc0403	Positive	0.55 ± 0.43	45.47 ± 17.61	3.44 ± 3.29	13.22
Panc1	Negative	1.70 ± 0.49	57.42 ± 11.56	175.57 ± 115.73	0.33

<sup>1</sup>IC<sub>50</sub> values for drug alone (SG3199), non-targeting PDC (SG3511) and  $\alpha\text{v}\beta 6$ -targeting PDC (SG3299) for targeting isogenic matched cell lines A375P-Puro and A375P-β6 and a panel of pancreatic cell lines (±SD, n=3). Cells were treated for 72h and subject to an MTT assay. <sup>2</sup>Ratio of mean IC<sub>50</sub> value for SG3511/SG3299.

## Results

### *In vitro* Studies Demonstrate $\alpha\text{v}\beta 6$ -Specific Cytotoxicity of SG3299

To create an  $\alpha\text{v}\beta 6$ -specific targeted therapy, we modified our FMDV-derived  $\alpha\text{v}\beta 6$ -specific peptide A20FMDV2 by addition of an N-terminal biotin, for antibody detection of the resulting conjugate, and addition of a C-terminal cysteine to permit conjugation to the payload tesirine (SG3249), which contains the drug SG3199 linked to a cathepsin B-cleavable linker. The resulting conjugate created an  $\alpha\text{v}\beta 6$ -specific peptide-drug conjugate (PDC) SG3299 (see below). A non-targeting (NT) peptide with a random sequence [7] and no RGD motif was conjugated to tesirine creating SG3511, which was used as a PDC control to SG3299. The sequences and structural diagrams of these peptides and PBD drug are shown in Supplementary Figure S1A. The purity of these peptides was assessed using high performance liquid chromatography-mass spectrometry (Supplementary Figure S1B and supplementary methods).

To confirm that the chemistry required to conjugate the linker-drug moiety to the peptide did not affect integrin specificity, we used flow cytometry with anti-biotin antibodies to measure conjugate binding to an isogenic matched pair of cell lines A375Ppuro and A375Pβ6, the latter engineered to overexpress  $\alpha\text{v}\beta 6$  [7]. Supplementary Figures S2A & S2B show that SG3299 exhibited dose-dependent binding to A375Pβ6 cells from 0.1 to 100 nM but failed to bind to A375Ppuro cells at even 100 nM. Mean fluorescence intensity (MFI) was used as a measure of binding.

In contrast, the control SG3511 failed to bind to either cell line at any concentration tested (100 nM dose shown). Thus, SG3299 retained specificity for  $\alpha\text{v}\beta 6$ .

Before proceeding to toxicity assays, we screened a panel of pancreatic cancer cell lines for endogenous  $\alpha\text{v}\beta 6$  expression and chose three positive (Capan-1,

Colo357, Panc0403) and one negative (Panc-1) cell line for study (Figure 1A). Figure 1B shows the dose response curves for the A375Ppuro/A375Pβ6 pair of cell lines when treated with NT-peptide, A20FMDV2, SG3199, SG3511 and SG3299. SG3299 was over 15-fold more potent in A375Pβ6 cells than SG3511 and was 5.7-fold more selective for A375Pβ6 cells than A375Ppuro cells as determined by IC<sub>50</sub> values (Table 1).

There was no significant difference in IC<sub>50</sub> values for the non-targeting SG3511 in A375Ppuro or A375Pβ6 cells, showing the non-selective toxicity of the NT-peptide-drug conjugate. Neither NT-peptide nor the modified A20FMDV2 had a significant effect on MTT activity (used as an indirect read out of cell proliferation) (Figure 1B).

To validate the toxic effects of the conjugates in pancreatic cancer cells endogenously expressing  $\alpha\text{v}\beta 6$ , we tested the panel of pancreatic cancer cell lines (Figure 1B and Table 1). Panc1 cells were included as an example of an  $\alpha\text{v}\beta 6$ -negative pancreatic cancer cell line. Panc1 showed limited toxic response to SG3299 compared with the other cell lines tested, but note, also showed a lower toxic response to the free drug. Capan-1 dose response curves are shown as an example of  $\alpha\text{v}\beta 6$ -positive pancreatic cancer cell response to the peptides and PDCs (Figure 1B). SG3299 was between 2.8- and 13.2-fold more selective for  $\alpha\text{v}\beta 6$ -positive pancreatic cells lines compared with SG3511, confirming that the anti-proliferative activity of SG3299 is more selective for  $\alpha\text{v}\beta 6$ -positive pancreatic cancer cells (Table 1).

### SG3299 is internalised only by $\alpha\text{v}\beta 6$ -Positive cells

The payload SG3199, must covalently bind to DNA to induce cytotoxicity [18]. To confirm internalisation of SG3299 was occurring in an  $\alpha\text{v}\beta 6$ -dependent manner, and thus delivering toxin SG3199 into the cell, we performed internalisation assays in Capan-1 cells. Figure 1C shows there was very little SG3511 associated with cells at 0' or 30' and that the actin cytoskeleton remained unchanged, suggesting no significant toxicity. In contrast, at 0' there was strong binding and entry into the cytoplasm by SG3299, but no SG3299 in the nuclei. At 30', the cells, which usually grow as tightly bound epithelial islands, had undergone significant morphological change, separated into individual cells with irregularly distributed actin, consistent with significant toxicity. Moreover, the green fluorescence was distributed throughout the whole cell by 30', confirming that SG3299 was throughout the cytoplasm and nuclei. Similar results were observed in other pancreatic cell lines (Supplementary Figure S2C). There was no significant difference in the levels

of internalised SG3299 or SG3511 in the  $\alpha v\beta 6$ -negative Panc1 cell line. Together, these data confirm that SG3299 binding and internalisation was  $\alpha v\beta 6$ -specific.

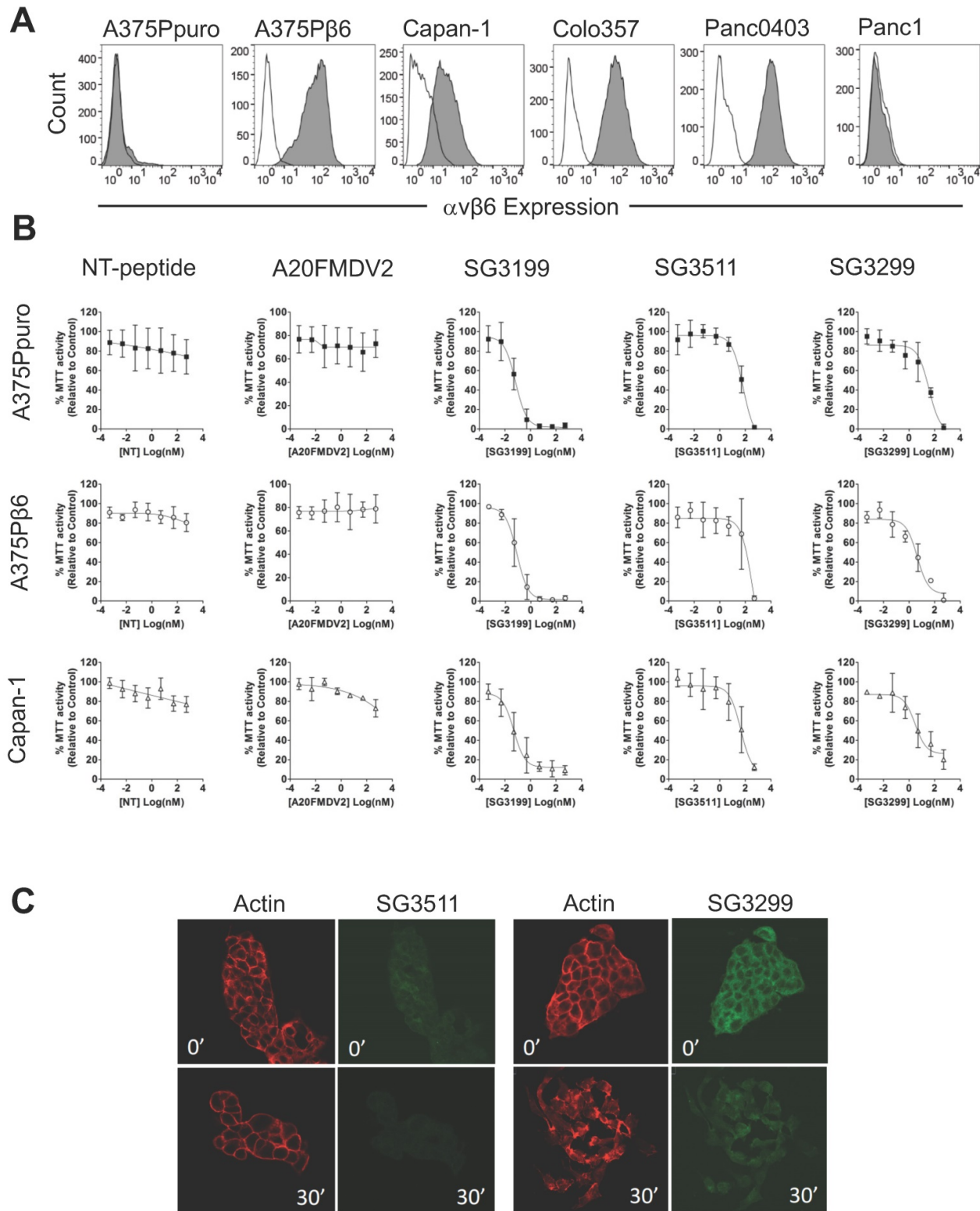


**Figure 1. SG3299 Selectively Kills  $\alpha v\beta 6$ -Expressing Cells.** **A**,  $\alpha v\beta 6$  expression of a panel of six cell lines using flow cytometry. Isotype control IgG is unshaded and gray shaded peaks represent  $\alpha v\beta 6$  expression. **B**, MTT growth inhibition assays were performed in the panel of cell lines in (A). Isogenic matched cell lines A375Ppuro and A375Pβ6 and  $\alpha v\beta 6$ -positive pancreatic cell line Capan-1 are shown as examples. Cells were treated with 0-500nM of non-targeting (NT) peptide,  $\alpha v\beta 6$ -specific peptide A20FMDV2, warhead only SG3199, NT-peptide conjugated to SG3249 (SG3511) and A20FMDV2 conjugated to SG3249 (SG3299) over 72h. All assays were performed in quadruplicate with a minimum of three biological repeats. **C**, Internalisation of SG3511 and SG3299 in Capan-1 cells. Cells were treated with 50nM SG3511 or SG3299 for 30 minutes on ice followed by incubation at 37°C. Indirect immunofluorescence was used to detect the biotin tag and Alexa-488 (green) conjugated secondary antibodies revealed the location of conjugates SG3511 and SG3299. The red fluorescence (Phalloidin-TRITC) shows the actin cytoskeleton at the same time-points.

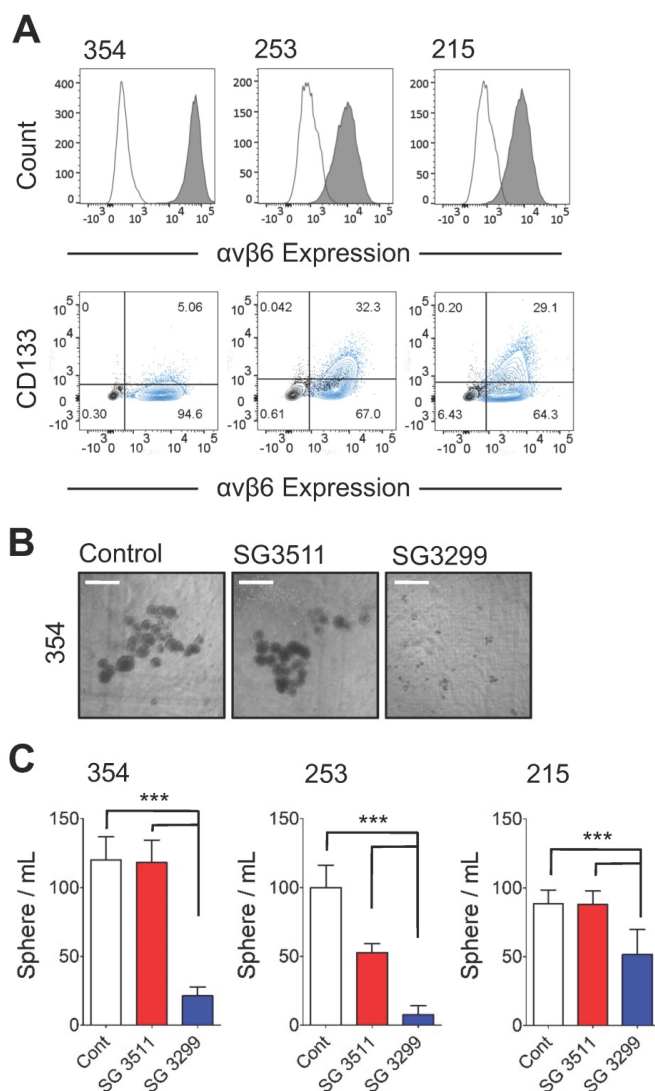


**Figure 2. SG3299 Inhibits Sphere Formation in  $\alpha v \beta 6$ -Expressing Patient-Derived Xenograft PDAC cells.** **A**,  $\alpha v \beta 6$  (upper panel) and CD133 expression of 354, 253 and 215 PDX PDAC cells using flow cytometry. Isotype control IgG is unshaded and gray shaded peaks represent  $\alpha v \beta 6$  expression. Lower panel, representative co-expression of CD133 and  $\alpha v \beta 6$  where the majority of CD133+ cells express  $\alpha v \beta 6$ . Isotype control is shown in black and the stained cell population in blue (n=2-5 replicates). **B**, Representative images of 354 cell spheres formed after 10 days culture following 3 days pre-treatment with Control (DMSO), NT-peptide SG3511 or SG3299 (1 nM) (X4 magnification, scale bar=500 $\mu$ m). **C**, Histograms quantifying the sphere formation assay shown in (B) (error bars represent standard deviation, n=5-6 wells/treatment). \*\*\*P<0.001 (relative to NT-peptide or SG3511 treatment arm).

### SG3299 inhibits sphere formation in $\alpha v \beta 6$ -expressing Patient-derived Xenograft PDAC cells

Cancer cells with 'stem-like' properties have been linked to tumor initiation, metastasis and development of resistance to therapy [24-26]. Formation of spheres *in vitro* that develop from individual cells is reported to enrich for the 'stem' cell phenotype in PDAC cells [20, 25]. Hence, to assess the ability of the PDCs to target PDAC cells with 'stem-like' properties, we performed a sphere-

forming assay. In preliminary experiments three patient-derived xenografts (PDX) cell populations (PANC354, PANC253 and PANC215; a kind gift from Dr Eshleman, John Hopkins University) were screened for  $\alpha v \beta 6$  and CD133 expression. Previous studies showed the tumour-initiating population of PDAC cells required CD133 expression [25]. The PDX cells were between 4.8%-31.1% positive for CD133 and also showed >90% expression of  $\beta 6$  (Figure 2A), and over 95% of CD133 cells were  $\alpha v \beta 6$ -positive. Next, the 354, 253 and 215 cells were subject to a sphere-forming assay. Prior to sphere formation, cells were treated for 3 days with the PDCs. Cells were then collected and re-seeded to form spheres. Representative images of 354 spheres after 10 days (from start of treatment) are shown in Figure 2B and quantified in Figure 2C (1 nM data shown as higher doses showed non-selective toxicity). Compared with control-treated spheres, SG3299 significantly reduced the number of spheres formed in all three cell models by 72 $\pm$ 27% (P<0.001). The non-targeting SG3511 also exhibited toxicity in 253 spheroids but SG3299 was still significantly more toxic than SG3511 (P<0.001).

### SG3299 selectively kills $\alpha v \beta 6$ -expressing pancreatic cancers *in vivo*

We confirmed the specificity of SG3299 to target and deliver the warhead SG3199 to  $\alpha v \beta 6$ -positive tumor cells *in vivo* by performing xenograft studies using cell lines A375Ppuro and A375P $\beta 6$  (Figures 3A & B) which are genetically identical apart from the expression of the  $\beta 6$  integrin subunit. Treatment commenced when tumors were ~100 mm<sup>3</sup> in all xenograft models. When compared with vehicle (PBS) treated mice, similar levels of tumor growth inhibition were observed in  $\alpha v \beta 6$ -negative A375Ppuro xenografts treated for 4 weeks with 10  $\mu$ g/kg tri-weekly intra-peritoneal (i.p) injections of non-targeting SG3511 versus  $\alpha v \beta 6$ -specific SG3299. Tumors (treated with SG3511 and SG3299 exhibited significant reductions in size (P<0.0001, 53.9 $\pm$ 23.7% and 34.8 $\pm$ 4.6% after 21 days respectively) but there was no significant difference in the effect of either treatment (P=0.24, after 30 days). These data suggest that SG3199 was delivered into  $\alpha v \beta 6$ -negative cells in a non-selective manner by both conjugates, possibly due to an inherent lipophilicity of SG3199 that acted independently of peptide specificity. In contrast, both SG3299 and SG3511 reduced A375P $\beta 6$  tumor growth compared with PBS treatment (79 $\pm$ 7% and 56.9 $\pm$ 16.2% respectively, P<0.0001) and SG3299 reduced growth by 2.3-fold more than SG3511 (P<0.0001) (Figure 3B). These data suggest that the specificity of SG3299 for  $\alpha v \beta 6$  increases the delivery of the cytotoxic warhead to  $\alpha v \beta 6$ -positive tumor cells. A20FMDV2 did not have

a significant effect on tumor growth in either A375Ppuro or A375P $\beta$ 6 xenograft model ( $P=0.24$ ).

We then assessed the efficacy of the PDCs using the Capan-1 PDAC xenograft model that endogenously expresses  $\alpha\beta$ 6. Capan-1 xenografts responded in a similar manner to A375P $\beta$ 6 xenografts upon 10  $\mu\text{g}/\text{kg}$  tri-weekly treatment, with significant growth inhibition with SG3511 and SG3299 ( $P<0.0001$ ) (Figure 3C). Again, SG3299 inhibited tumor growth significantly more than SG3511 ( $P<0.0001$ ).

To investigate whether a higher treatment dose would be even more efficacious in this PDAC model, we repeated the Capan-1 xenograft study with an increased dosage of 25 $\mu\text{g}/\text{kg}$  but only bi-weekly for 4 weeks (Figure 3D). This dosage was tolerated by mice in preliminary studies (data not shown). Again, SG3299 significantly reduced Capan-1 tumor growth achieving 97.7 $\pm$ 2% ( $P<0.0001$ ) and 96.1 $\pm$ 3.4% ( $P<0.0001$ ) reductions compared to PBS and SG3511, respectively. A20FMDV2 again had no significant effect on tumor growth. The higher dosage of SG3299 eliminated tumors in 4 out of 5 mice and the one remaining tumor was less than 25 $\text{mm}^3$  after 30 days. Several mice receiving this dosing regimen were monitored for survival analysis (Figure 3E). SG3299 treatment conferred a significant survival advantage compared to all other treatments ( $P<0.043$ ), where all mice were alive after 130 days (4/5 were cured) compared with median survival of 71.5, 62.5 and 95 days for PBS, A20FMDV2 and SG3511-treated mice respectively. Thus, SG3299 significantly prolongs survival of mice bearing Capan-1 xenografts.  $P<0.0001$ ).

To confirm that intraperitoneal injection of SG3299 could deliver effective levels of PDC to the blood and thus elicit a therapeutic effect on tumour xenografts *in vivo*, we developed an ELISA to detect the serum concentration of SG3299. Capture of the PDC via the C-terminal PBD and subsequent detection via the N-terminal biotin tag allowed us to detect the concentration of intact SG3299 molecules with a sensitivity as low as 0.5nM (Supplementary Figure S3A and S3B). Mice were injected with an acute dose of 20  $\mu\text{g}/\text{kg}$  SG3299 and serum samples isolated between 2 and 60 minutes. The concentration of SG3299 in the serum increased over 60 minutes of treatment up to approximately 28nM, well above the effective dose of SG3299 against  $\alpha\beta$ 6-positive PDAC cells we determined *in vitro* (Table 1). No SG3299 was detected in the urine in the same time frame (data not shown). Thus, intact SG3299 is delivered effectively to the blood and maintained for at least 60 minutes after treatment, indicating that therapeutically active SG3299 is bioavailable following i.p. injection.

### **SG3299 treatment reduced proliferation and induced DNA damage and apoptosis in pancreatic tumors**

To investigate the molecular effects of PDC therapy on Capan-1 tumors at a cellular level, we harvested Capan-1 xenografts ( $n=3/\text{treatment}$ ) from the xenograft study shown after 3 peptide-drug treatments (tumors for immunochemistry were harvested on day 11, Figure 3D). Immunohistochemistry was performed for a panel of markers to detect DNA damage ( $\gamma\text{H2AX}$ ), residual epithelial cells (cytokeratin (CK) and E-cadherin), proliferation (Ki67),  $\alpha\beta$ 6, apoptosis (cleaved-caspase3), and endothelial cells as a measure of blood vasculature (endomucin), stromal fibroblasts (vimentin) and activated fibroblasts ( $\alpha\text{-sma}$ ). Tumors were harvested at this time point to provide enough tissue for analysis. The growth curves for the harvested tumors are shown in Supplementary Figure S4A.

No adverse effects were observed with either PDC treatment, as shown by stable mouse weight (Supplementary Figure S4B), normal animal behaviour and by the absence of gross histological change in lung, intestine and stomach (Supplementary Figure S4C-E), three tissues we previously have reported that express endogenous  $\alpha\beta$ 6 in mice [7].

Representative photomicrographs of immunohistochemical staining are shown (Figure 4A) and were quantified using VisioPharm image analysis software (Figure 4B). There was a significant reduction in proliferation (as determined by reduced Ki67 staining) with SG3299 treatment compared with control (67.5 $\pm$ 15%;  $P<0.01$ ) and compared with SG3511 (66.2 $\pm$ 15.7%;  $P<0.01$ ). This was associated with a marked increase in DNA damage (as measured by 5.9-fold increase in  $\gamma\text{H2AX}$ ) and a reduction in  $\alpha\beta$ 6 expression of 2.2-fold (54 $\pm$ 32.9%) caused by SG3299 treatment compared with PBS (control) treated tumors (Figure 4B).

Compared with PBS (control) treatment, SG3299 was the only treatment to dramatically change tumor composition. For example, compared with PBS (control) treatment there was a significant reduction in CK-positive (79.2 $\pm$ 11.2%;  $P<0.001$ ) and E-cadherin-positive (85 $\pm$ 8% ( $P<0.01$ )) epithelial cells. These observations correlated with a marked increase in DNA damage ( $\gamma\text{H2AX}$ ) and a significant increase in apoptosis as measured by cleaved-caspase 3 (5.8-fold increase from PBS,  $P<0.001$ ), significantly increased vimentin (4.6-fold compared with PBS,  $P<0.01$ ) and significantly increased  $\alpha\text{-sma}$  expression (1.9-fold increase from PBS,  $P<0.01$ ) (Figure 4B). Thus SG3299-treated Capan-1 tumors became mostly stromal fibroblasts after just 3 treatments with the peptide-drug SG3299.

Non-targeting SG3511 also produced a significant increase in apoptosis and DNA damage ( $P < 0.05$ ) again, probably as a result of the inherent lipophilicity of tesirine, but there was no significant change in tumor cell number, as measured by tumour cell area, CK-expression and confirmed with E-cadherin expression. A20FMDV2 did not elicit any significant tumor changes compared with PBS control treatment as determined by this panel of markers.

**SG3299 selectively kills  $\alpha\text{v}\beta 6$ -expressing pancreatic cancers grown with stellate cells *in vivo***

PDAC tumours are characterised as having a high fraction of stroma rich in pancreatic stellate cells

and mouse models should reflect this pathology [26]. To validate the efficacy of the PDC SG3299 in a model that more closely reflects the human disease, we treated mice bearing tumors formed of a second  $\alpha\text{v}\beta 6$ -positive PDAC cell line model, Panc0403, co-injected with human pancreatic stellate cells PS1 in a ratio of Panc0403:PS1 of 1:2. SG3299 significantly reduced Panc0403/PS1 xenograft tumor growth by  $75.8 \pm 6\%$  ( $P < 0.001$ ) compared with PBS treatment and by  $60.4 \pm 9.8\%$  ( $P < 0.05$ ) compared with SG3511 therapy (Figure 5A). Notably, Panc0403/PS1 tumour growth rate remained suppressed by SG3299 therapy even after treatment had ceased (Supplementary Figure S5).

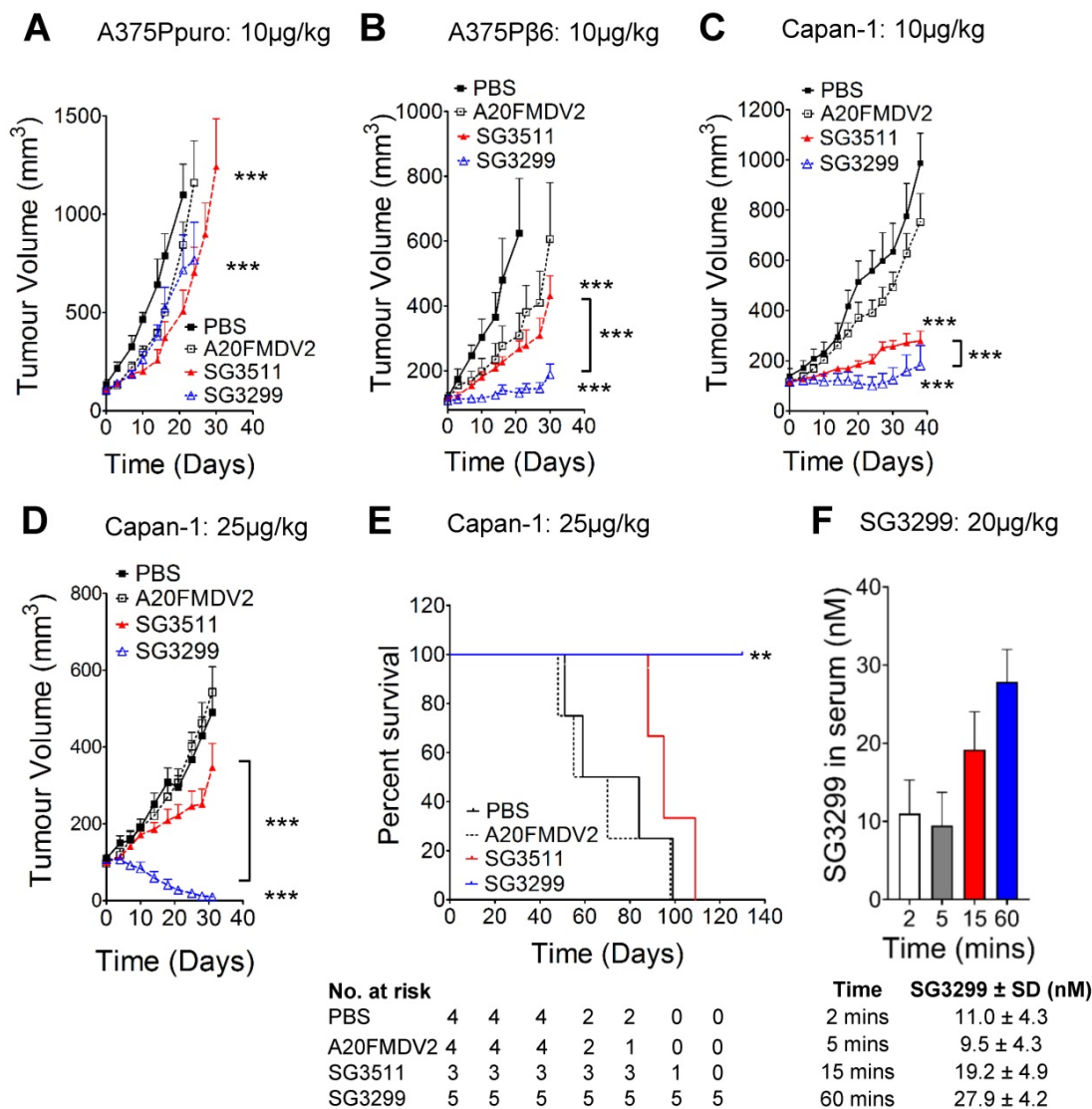


**Figure 3. SG3299 Selectively Kills  $\alpha\text{v}\beta 6$ -Expressing Cancers *In Vivo*.** **A**, Athymic CD1Nu/Nu female mice bearing human A375Ppuro **or B**, A375Pβ6 xenograft tumours were treated with PBS (black square), A20FMDV2 (unfilled square), SG3511 (red filled triangle) or SG3299 (blue unfilled triangle) (10µg/kg; i.p administration) thrice weekly for 4 consecutive weeks (start of treatment day 0). **C**, Mice bearing human Capan-1 tumours were treated as in (A&B) for 5 weeks **or D**, with 25 µg/kg bi-weekly for 4 weeks. Data are presented as mean tumor volume (error bars represent SEM, n=6-8 mice/group). Treatment commenced when tumors reached 100 mm<sup>3</sup>. **E**, Kaplan Meier survival plot of mice from D (excluding mice harvested for immunohistochemical analyses). \* $P < 0.05$ , \*\* $P < 0.01$ , \*\*\* $P < 0.001$  (relative to NT-peptide or indicated treatment arm). **F**, Mice were treated with an acute dose of 20 µg/kg SG3299 administered by i.p. injection for 2, 5, 15 or 60 minutes. The concentration of SG3299 in the blood at each time point was determined by ELISA. Data are presented as mean ± SD, n=2-4 mice/group.

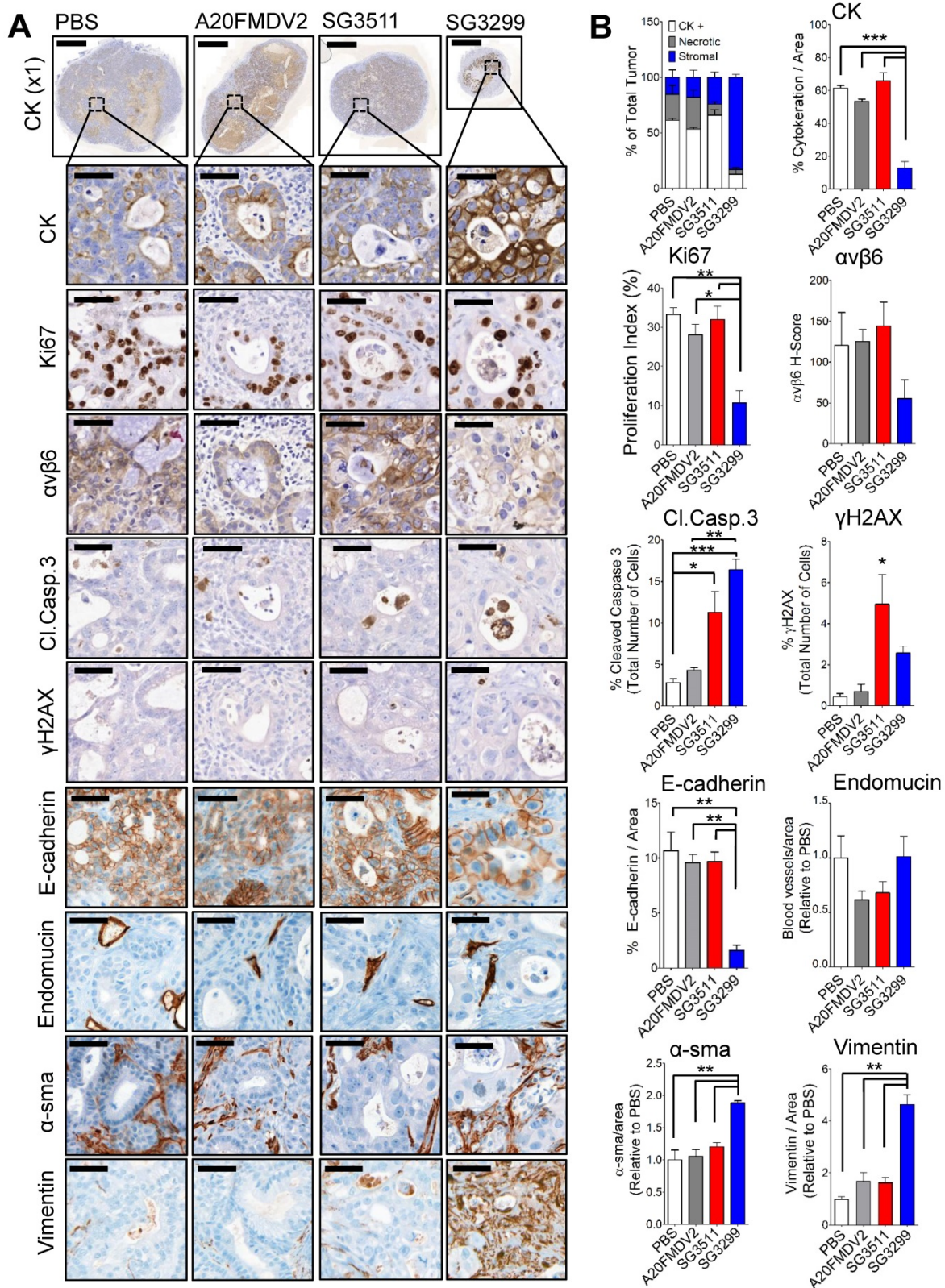


**Figure 4. SG3299 Treatment Reduces Pancreatic Tumor Growth by inducing DNA Damage and Apoptosis.** **A**, Micrographs of Capan-1 tumor xenografts from mice treated with NT-peptide, A20FMDV2, SG3511 or SG3299 (25 µg/kg; i.p administration) bi-weekly for 10 days (3 treatments) (n=3/treatment tumors harvested after 10 days treatment from Figure 3D). Tumors were harvested, fixed, paraffin-embedded and sections subject to immunohistochemical staining for the indicated molecules of interest including pan-cytokeratin (CK, epithelial marker), Ki67 (proliferation), αβ6, cleaved-caspase 3 (Cl.caspase 3; apoptosis), E-cadherin (epithelial marker), blood vasculature (endomucin), activated fibroblasts/ stellate cells (α-sma and vimentin), and γH2AX (DNA damage/adduct formation). Representative images are shown of the 3 tumors harvested for each treatment. Magnification bar=2000 µm for x1 magnification images, magnified images (x50) are of indicated region of interest (tumor cells), with a scale bar of 50 µm. **B**, Bar graph of tissue composition of xenografts (% CK+ cells=white bar, % necrotic area in gray and % stroma is in blue) and histograms of marker expression shown in (A). Staining assessed & scored by 2 individuals or using VisioPharm computational analysis software (n=3 individual tumors, error bars represent SEM). \*P<0.05, \*\*P<0.01, \*\*\*P<0.001 (relative to PBS or indicated treatment).

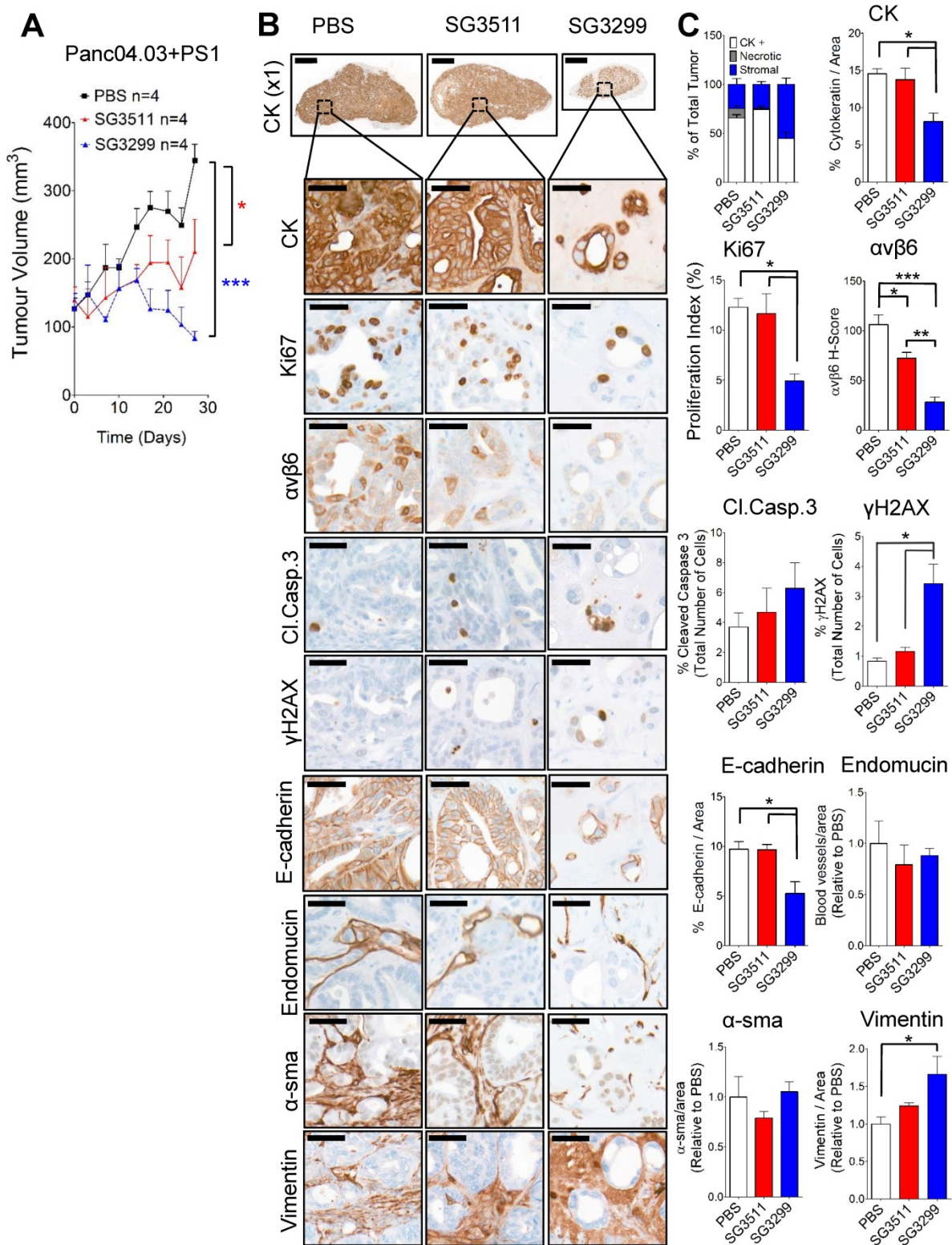


**Figure 5. Pancreatic stellate cells do not prevent the anti-tumorigenic action of SG3299.** **A**, Athymic CD1Nu/Nu female mice bearing human Panc0403+PS1 xenograft tumours were treated with NT-peptide (black square), SG3511 (red filled triangle) or SG3299 (blue unfilled triangle) (20 µg/kg; i.p administration) bi-weekly for 4 consecutive weeks (start of treatment day 0). Data are presented as mean tumor volume (error bars represent SEM, n=4 mice/group). Treatment commenced when tumors reached 100 mm<sup>3</sup>. **B**, Micrographs of Panc0403+PS1 tumor xenografts from mice treated as in (A) (n=4/treatment, after 4 weeks treatment). Tumors were harvested, fixed, paraffin-embedded and sections subject to immunohistochemical staining for the indicated molecules of interest including pan-cytokeratin (CK, epithelial marker), Ki67 (proliferation), αvβ6, cleaved-caspase 3 (Cl.Caspase 3; apoptosis), E-cadherin (epithelial marker), blood vasculature (endomucin), activated fibroblasts (α-sma), vimentin (stroma) and γH2AX (DNA damage/adduct formation). Representative images are shown of the 4 tumors harvested for each treatment. Magnification bar=2000 µM for x1 magnification images, magnified images (x50) are of indicated region of interest (tumor cells), with a scale bar of 50µM. **C**, Bar graph of composition of xenografts (% CK+ cells=white bar, % necrotic area in gray and % stroma is in blue) from (A) and histograms of marker expression shown in (B). Staining assessed & scored by 2 individuals or using VisioPharm computational analysis software (n=4 individual tumors, error bars represent SEM). \*P=0.05, \*\*P=0.01, \*\*\*P<0.001 (relative to PBS or indicated treatment).

### **SG3299 treatment induced DNA damage and caused reduced proliferation and apoptosis in Panc0403/PS1 pancreatic tumors**

As per Capan-1 xenograft studies, SG3299 was the only treatment to dramatically change tumor composition. SG3299 significantly increased DNA damage ( $\gamma$ H2AX) by 5.5-fold and 2.9-fold ( $P < 0.05$ ) compared with PBS and SG3511 respectively (Figure 5B & C). As a likely consequence of this, SG3299 significantly reduced proliferation (Ki67) by  $60 \pm 13.1\%$  ( $P < 0.05$ ) and  $54.8 \pm 13.8\%$  ( $P < 0.05$ ) compared with PBS and SG3511 respectively. SG3299 also significantly reduced epithelial cell number (as measured by CK and E-cadherin) compared with PBS and SG3511 ( $44.2 \pm 18.1\%$  and  $41.2 \pm 19.1\%$  reductions respectively for CK;  $46 \pm 11\%$  and  $32.1 \pm 34.6\%$  reductions respectively for E-cadherin,  $P < 0.05$ ).  $\beta 6$  expression was also significantly reduced with SG3299 treatment by  $73.4 \pm 11\%$  ( $P < 0.001$ ) compared to PBS and  $61.1 \pm 16.1\%$  ( $P < 0.01$ ) compared to SG3511.

### **Discussion**

Patients with pancreatic cancer are in desperate need of therapies that are more effective than the non-specific cytotoxic drugs currently available. Integrin  $\alpha \beta 6$  represents an exciting biomarker and therapeutic target in pancreatic cancer, especially as it was found to be highly expressed in almost 100% of PDAC cases tested [12-14], including the paired metastases [12]. In this study we wished to develop a peptide-drug conjugate to treat pancreatic cancer.

Peptides are attractive for use as anti-cancer therapies as they are small, easy to synthesise and modify, have good biocompatibility and are more easily able to penetrate tumors than antibodies [19]. Peptides are also rapidly excreted [27], thereby removing rapidly from the body any unused drug conjugated to the peptide, limiting toxicity to normal tissues. Additionally, the costs of treating patients with antibodies can be prohibitive [28, 29] whereas PDCs can offer a more favourable financial option. The observation that FMDV infects cattle using bovine  $\alpha \beta 6$  [30] led us to successfully identify A20FMDV2, a 20mer peptide that retained the integrin-specificity of the whole virus and the functionality, since A20FMDV2 binding promotes  $\alpha \beta 6$ -dependent internalisation into cells [7, 15, 16]. Our study shows that  $\alpha \beta 6$ -specific peptide-drug conjugate SG3299 is an effective molecular-specific therapy for three different  $\alpha \beta 6$ -expressing tumour models including two PDAC xenografts.

PDCs have already been tested clinically in other cancers. Advanced endometrial (ZoptEC; NCT01767155), metastatic hormone-resistant prostate (NCT01240629) and metastatic breast and lung cancer (GRABM-

B; NCT01480583 and GRABM-L; NCT01497665) have all received PDC therapies. However, none of these trials targeted a cancer-expressed antigen. These trials targeted the Leutenizing Releasing Hormone (LHRH) receptor, GnRH-R or the low density lipoprotein receptor-related protein 1 (LRP-1). The Phase 3 endometrial and Phase 2 GRABM-B trials failed to discern any survival benefit between standard of care and the PDCs combined with standards of care and thus the trials were terminated. These data suggest the choice of target for PDCs, as for any anti-cancer therapy, is key in the efficacy of the PDCs and emphasises the potential value of  $\alpha \beta 6$  as a cancer-specific target.

The choice of warhead of PDCs is also critical in their likely success. PBD toxins, unlike other forms of chemotherapy, covalently cross-link both DNA strands simultaneously [18]. This DNA inter-strand cross-link effectively blocks the division of cancer cells without distorting the structure of the DNA helix, thus avoiding triggering the DNA repair process and results in a longer duration of the cytotoxic effect [31]. The cytotoxic effect of SG3299 requires DNA damage and this was observed in two different models of PDAC. This correlated with increased apoptosis and the associated reduction in tumour size and tumour cell proliferation. In agreement with these observed effects of SG3299, the data showed that after only three therapeutic treatments the Capan-1 tumour was mostly stromal fibroblasts (Figure 4).

The biology of pancreatic adenocarcinoma has suggested there are key components that must be targeted for any therapy to be effective. Thus, some PDAC cancer cells have been reported to possess 'stem-like' properties, associated with tumor initiation, metastasis and therapeutic resistance [24-26]. Over 95% of the CD133-positive 'tumour initiating' cells in the PDAC PDX models used here were found to be  $\alpha \beta 6$ -positive (Figure 2A), suggesting targeting the  $\alpha \beta 6$ -positive population also targets the 'tumour initiating' cells. Data show that growing three-dimensional 'spheres' from individual PDAC cells *in vitro* enriches for the 'stem-like' phenotype [25]. As SG3299 significantly reduced sphere-formation from PDAC PDX cells the results suggest these 'stem-like' cells are susceptible to SG3299. These findings are supported by previous studies where an antibody-PBD drug conjugate successfully eradicated tumor-initiating cells [32]. Moreover, it is well established that PDAC tumours are mostly desmoplastic, formed predominantly of pancreatic stellate cells and their secreted stromal protein rich in collagen [33]. Other data suggest that the pancreatic stellate cells may also promote drug resistance in pancreatic cancer [34]. Therefore, we

treated tumors formed from Panc0403 co-injected with human pancreatic stellate cells to mimic the human disease. Results showed that the presence of stellate cells did not inhibit the cytotoxic effect of SG3299, which still showed a strong therapeutic effect (Figure 5). Thus both 'stem-like' PDAC cells and pancreatic stellate cells do not prevent  $\alpha\beta6$ -specific SG3299 mediating a significant therapeutic effect.

A previous study showed good evidence that  $\alpha\beta6$  functioned as a tumor suppressor in a transgenic mouse model of PDAC [35]. This is in contrast to data in breast, cervix, colon and lung [8-11] suggesting  $\alpha\beta6$  functions as a tumor promotor, reducing the survival of patients that have cancers over-expressing this integrin. By using  $\alpha\beta6$  as a therapeutic target to selectively kill all  $\alpha\beta6$ -expressing tumor cells, this apparent contradiction becomes irrelevant. Our data show that SG3299 can achieve that goal.

A new radiotracer, fluorine-18 radiolabelled A20FMDV2, was tested in clinical trials for detection of  $\alpha\beta6$  as part of an idiopathic pulmonary fibrosis (IPF) trial (NCT02612051). As  $\alpha\beta6$  is expressed in a wide range of malignancies, including pancreatic cancer [7,12], F18-A20FMDV2 or other recently described  $\alpha\beta6$ -targeting radiotracers including from Hausner et al [36] and the cystine-knot R01 variant from the Gambhir Laboratory (Clinical Trials No. NCT02683824), offer non-invasive means of stratifying patients who may be eligible to receive anti- $\alpha\beta6$  therapy. Promisingly SG3299 anti-cancer therapy showed no gross adverse effects in mouse weight, mouse behaviour or histologically in three different tissues that we previously have reported expressed  $\alpha\beta6$  in mice (reference 7 and Supplementary Figure S4); these data confirm that SG3299, targeting  $\alpha\beta6$ , functioned as a cancer-specific therapy [37]. The data also showed that when the dose and dosing schedule are optimal, SG3299 can be curative and a similar optimisation is likely to be critical for successful translation to humans. SG3299 has the potential to be therapeutically effective in PDAC and provide the first molecular-specific treatment for pancreatic cancer.

We have successfully translated the biological behaviour of the foot-and-mouth-disease virus into an effective anti-cancer therapy for human pancreatic cancer, and hopefully other types of cancer. With our development of  $\alpha\beta6$ -specific peptide-drug conjugates such as SG3299, and the development of human [38] and humanised (trial ID NCT01371305)  $\alpha\beta6$ -blocking antibodies, it is clear that specific targeting  $\alpha\beta6$  in humans is now a practical possibility and should become a platform for development of improved therapies for the effective treatment of pancreatic and hopefully many other types of cancer.

## Abbreviations

$\alpha$ -sma: alpha smooth muscle actin; CK: cytokeratin; DMSO: dimethyl sulfoxide; FMDV: foot-and-mouth-disease virus; PDAC: pancreatic ductal adenocarcinoma; PBS: phosphate buffered saline; PDC: peptide drug conjugates; SD: standard deviation.

## Supplementary Material

Supplementary methods and figures.

<http://www.thno.org/v10p2930s1.pdf>

## Acknowledgements

Kind thanks to several Core Services at Barts Cancer Institute, including the Animal Technical Service, Histopathology, Flow Cytometry and Microscopy, which are all funded by a Cancer Research UK Centre grant. Kind thanks also to Professor James Eshleman (John Hopkins University, USA) for his generous gift of the 354, 253 and 215 PDAC PDX cells.

## Funding

This research was funded by ADC Therapeutics, Pancreatic Cancer Research Fund and a Cancer Research UK Centre grant (C16420/A18066).

## Author Contributions

Conception and design: J. F. Marshall, K. M. Moore and A. Desai. Development of methodology: K. M. Moore, A. Desai, B. de Luxán Delgado, S. M. D. Trabulo, E.R. Murray, J. F. Marshall. Acquisition of data: K. M. Moore, A. Desai, B. de Luxán Delgado, S. M. D. Trabulo, C. Reader, N. F. Brown, E.R. Murray. Analysis and interpretation of data: K. M. Moore, A. Desai, E.R. Murray, A. Brentnall, J. F. Marshall. Writing, reviewing project & manuscript: J. F. Marshall, K. M. Moore, A. Desai, E.R. Murray, A. Brentnall, L. Masterson, F. Zammarchi, P. van Berkel, J. Hartley, P. Howard. Study supervision and funding: J. F. Marshall. Material manufacture and quality control: Luke Masterson.

## Competing Interests

Philip Howard, Francesca Zammarchi, Patrick H. van Berkel and John A. Hartley are employees and/or shareholders of ADC Therapeutics. All other authors declare no conflicts of interest.

## References

1. Siegel R, Ma J, Zou Z and Jemal A. Cancer statistics 2014. *CA Cancer J Clin* 2014; 64: 9-29.
2. Thomas JK, Kim MS, Balakrishnan L, Nanjappa V, Raju R, Marimuthu A, et al. Pancreatic cancer database: an integrative resource for pancreatic cancer. *Cancer Biol Ther*. 2014;15:963-967.

3. Conroy T, Gavaille C, Samalin E, Ychou M, Ducreux M. The role of the FOLFIRINOX regimen for advanced pancreatic cancer. *Curr Oncol Rep*. 2013; 15: 182-189.
4. Conroy T, Desseigne F, Ychou M, Bouché O, Guimbaud R, Bécouarn Y, et al. FOLFIRINOX versus gemcitabine for metastatic pancreatic cancer. *N Engl J Med*. 2011; 364: 1817-1825.
5. Rahib L, Smith BD, Aizenberg R, Rosenzweig AB, Fleshman JM, Matrisian LM. Projecting cancer incidence and deaths to 2030: the unexpected burden of thyroid, liver and pancreas cancers in the United States. *Cancer Res*. 2014; 74: 2913-2921
6. Barczyk M, Carracedo S, and Gullberg D. Integrins. *Cell Tissue Res*. 2012; 339: 269-280
7. Saha A, Ellison D, Thomas GJ, Vallath S, Mather S J, Hart IR. et al. High-resolution in vivo imaging of breast cancer by targeting the pro-invasive integrin alphavbeta6. *J Pathol*. 2010; 222: 52-63.
8. Moore KM, Thomas GJ, Duffy SW, Warwick J, Chou P, Ellis IO, et al. Therapeutic Targeting of Integrin  $\alpha v \beta 6$  in Breast Cancer. *J Natl Cancer Inst* 2014; 106 (8). pii:dju 169. Doi: 10.1093/jnci/dju 169
9. Hazelbag S, Kenter GG, Gorter A, Dreef EJ, Koopman LA, Violette SM et al. Overexpression of the  $\alpha v \beta 6$  integrin in cervical squamous cell carcinoma is a prognostic factor for decreased survival. *J Pathol*. 2007; 212: 316-324
10. Bates RC, Bellovin DI, Brown C, Maynard E, Wu B, Kawakatsu H, et al. Transcriptional activation of integrin beta6 during the epithelial-mesenchymal transition defines a novel prognostic indicator of aggressive colon carcinoma. *J Clin Invest* 2005;115: 339-347.
11. Elayadi AN, Samli KN, Prudkin L, Liu YH, Bian A, Xie XJ, et al. A peptide selected by biopanning identifies the integrin alphavbeta6 as a prognostic biomarker for nonsmall cell lung cancer. *Cancer Res*. 2007; 67: 5889-5895.
12. Reader CS, Vallath S, Steele CW, Haider S, Brentnall A, Desai A et al. The integrin  $\alpha v \beta 6$  drives pancreatic cancer through diverse mechanisms and represents an effective target for therapy. *J Pathol*. 2019; 249:332-342.
13. Sipos B, Hahn D, Carceller A, Piulats J, Kaltoff H, Goodman SL, et al. Immunohistochemical screening for  $\beta 6$ -integrin subunit expression in adenocarcinomas using a novel monoclonal antibody reveals strong up-regulation in pancreatic ductal adenocarcinomas in vivo and in vitro. *Histopathology*. 2004; 45: 226-236.
14. Steiger K, Schlitter A-M, Weichert W, Esposito I, Wester H-J, Notni J. Perspective of  $\alpha v \beta 6$ -integrin imaging for clinical management of pancreatic carcinoma and its precursor lesions. *Mol Imaging*. 2017; 16:1-3
15. DiCara D, Rapsarda C, Sutcliffe JL, Violette SM, Weinberg PH, Hart IR et al. Structure-function analysis of Arg-Gly-Asp helix motifs in alpha v beta 6 integrin ligands. *J Biol Chem*. 2007; 282: 9657-9665.
16. John AE, Luckett JC, Tatler AL, Awais RO, Desai A, Habgood A, et al. Preclinical SPECT/CT imaging of  $\alpha v \beta 6$  integrins for molecular stratification of idiopathic pulmonary fibrosis. *J Nucl Med*. 2013; 54: 2146-52.
17. Tiberghien AC, Levy JN, Masterson LA, Patel NV, Adams LR, Corbett S. et al. Design and Synthesis of Tesirine, a Clinical Antibody-Drug Conjugate Pyrrolbenzodiazepine Dimer Payload. *ACS Med Chem Lett* 2016; 7:983-987.
18. Hartley JA, Flynn MJ, Bingham JP, Corbett S, Reinert H, Tiberghien A, et al. Pre-clinical pharmacology and mechanism of action of SG3199, the pyrrolbenzodiazepine (PBD) dimer warhead component of antibody-drug conjugate (ADC) payload tesirine. *Sci Rep*. 2018; 8:10479.
19. Rudin CM, Pietanza MC, Bauer TM, Ready N, Morgensztern D, Glisson BS et al. Rovalpituzumab tesirine, a DLL3-targeted antibody-drug conjugate, in recurrent small-cell lung cancer: a first-in-human, first-in-class, open-label, phase I study. *Lancet Oncol*, 2017; 18: 42-51.
20. Cioffi M, Trabulo S, Hidalgo M, Costello E, Greenhalf W, Erkan M et al. Inhibition of CD47 Effectively Targets Pancreatic Cancer Stem Cells via Dual Mechanisms. *Clin Cancer Res*. 2015; 21:2325-2337
21. Flynn MJ, Zammarchi F, Tyrer PC, Akarca AU, Janghra N, Britten CE et al. ADCT-301, a pyrrolbenzodiazepine (PBD) dimer-containing antibody drug conjugate (ADC) targeting CD25-expressing hematological malignancies. *Mol Cancer Ther*. 2016;15:2709-2721
22. Crowder MJ and Hand DJ. Analysis of Repeated Measures (First edition). Monographs on Statistics and Applied Probability. London, UK; Chapman & Hall: 1990.
23. R Development Core Team. R: A Language and Environment for Statistical Computing. Vienna, Austria: R Foundation for Statistical Computing. ISBN 3-900051-07-0. 2010.
24. Kreso A, Dick JE. Evolution of the cancer stem cell model. *Cell Stem Cell*. 2014; 14: 275-291.
25. Hermann PC, Huber SL, Herrler T, Aicher A, Ellwart JW, Guba M. et al. Distinct populations of cancer stem cells determine tumor growth and metastatic activity in human pancreatic cancer. *Cell Stem Cell*. 2007; 1; 313-323.
26. Mueller MT, Hermann PC, Witthauer J, Rubio-Viqueira B, Leicht SF, Huber S. et al. Combined targeted treatment to eliminate tumorigenic cancer stem cells in human pancreatic cancer. *Gastroenterology*. 2009; 137; 1102-1113.
27. Hausner SH, Abbey CK, Bold RJ, Gagnon MK, Marik J, Marshall JF, et al. Targeted in vivo imaging of integrin  $\alpha v \beta 6$  with an improved radiotracer and its relevance in a pancreatic tumor model. *Cancer Res*. 2009; 69: 5843-4410.
28. Fosgerau, K. and Hoffmann, T. Peptide therapeutics: current status and future directions. *Drug Discov Today*. 2015; 20:122-128.
29. Prasad V, De Jesus K, Mailankody S. The high price of anticancer drugs: origins, implications, barriers, solutions. *Nat Rev Clin Onc*. 2017;14:381-390.
30. Jackson T, Sheppard D, Denyer M, Blakemore W, King AM. The epithelial integrin alphavbeta6 is a receptor for foot-and-mouth-disease virus. *J Virol*. 2000; 74:4949-4956
31. Hartley, J.A. The development of pyrrolbenzodiazepines as antitumour agents. *Expert Opin Investig Drugs*, 2011; 20: 733-44.
32. Saunders LR, Bankovich AJ, Anderson WC, Aujay MA, Bheddah S, Black K, et al. A DLL3-targeted antibody-drug conjugate eradicates high-grade pulmonary neuroendocrine tumor-initiating cells in vivo. *Sci Trans Med*. 2015; 7: 302ra136.
33. Olive KP, Jacobetz MA, Davidson CJ, Gopinathan A, McIntyre D, Honess D, et al. Inhibition of Hedgehog signaling enhances delivery of chemotherapy in a mouse model of pancreatic cancer. *Science*. 2009; 324: 1457-1461.
34. Carapuça EF, Gemenetizidis E, Feig C, Bapiro TE, Williams MD, Wilson AS, et al. Anti-stromal treatment together with chemotherapy targets multiple signalling pathways in pancreatic adenocarcinoma. *J Pathol*. 2016; 239:286-296.
35. Hezel AF, Deshpande V, Zimmerman SM, Contino G, Alagesan B, O'Dell MR et al. TGF-beta and alphavbeta6 integrin act in a common pathway to suppress pancreatic cancer progression. *Cancer Res*. 2012; 72: 4840-4845.
36. Hausner SH, Bold RJ, Cheuy LY, Chew HK, Daly ME, et al. Preclinical development and first-in-human imaging of the integrin  $\alpha v \beta 6$  with [18F] $\alpha v \beta 6$ -binding peptide in metastatic carcinoma. *Clin Cancer Res*. 2019; 25: 1206-1215.
37. Breuss JM, Gallo J, DeLisser HM, Klimanskaya IV, Folkesson HG, Pittet JF, et al. Expression of the beta 6 integrin subunit in development, neoplasia and tissue repair suggests a role in epithelial remodeling. *J Cell Sci*. 1995; 108: 2241-2251.
38. Eberlein C, Kendrew J, McDaid K, Alfred A, Kang JS, Jacobs VN, et al. A human monoclonal antibody 264RAD targeting alphavbeta6 integrin reduces tumour growth and metastasis and modulates key biomarkers in vivo. *Oncogene*. 2013; 32: 4406-4416.